

Utility of Respiratory-Navigator-Rejected k-Space Lines for Improved Signal-to-Noise Ratio in Three-Dimensional Cardiac MR

Mehmet Akçakaya, Jaime L. Shaw, Thomas H. Hauser, and Reza Nezafat*

Purpose: To develop and evaluate a technique that uses the k-space lines rejected by prospective respiratory navigator (NAV) to improve the signal-to-noise ratio (SNR) without increasing the scan time.

Methods: In conventional image reconstruction, the motion-corrupted k-space lines rejected by the NAV are not used. In this study, a set of translational motion parameters for the NAV-rejected lines and a phase-corrected average for the k-space line are estimated jointly using a maximum-likelihood approach and the information from the corresponding accepted k-space lines. Left coronary artery images were acquired in 10 healthy adult subjects, and the proposed approach incorporating the NAV-rejected lines was compared with the conventional dataset with NAV-accepted lines only, as well as a simple average of all k-space lines, in terms of SNR, normalized vessel sharpness and qualitative image scores on a four-point scale (1 = poor, 4 = excellent). Late gadolinium enhancement images of the left atrium were also acquired in 21 patients with atrial fibrillation pre- or post-pulmonary vein isolation. Images reconstructed with the proposed, conventional, and simple averaging methods were compared in terms of SNR, and subjective image quality on a four-point scale.

Results: For coronary MRI, there was a significant improvement in SNR with the proposed technique, but no significant difference in normalized vessel sharpness or qualitative image scores were observed with respect to the conventional method. Simple averaging resulted in an SNR gain, but significant loss in vessel sharpness and image quality. For late gadolinium enhancement, there was a significant increase in SNR, but no significant differences were observed in subjective image quality scores between the proposed and conventional methods. There was an SNR gain, but image quality loss for simple averaging, when compared with the conventional technique. In both coronary MRI and late gadolinium enhancement, the SNR gain of the proposed method was not significantly different than the maximum theoretical SNR gain.

Conclusion: The proposed technique improves SNR using the additional information from NAV-rejected k-space lines, while providing similar image quality to standard reconstruction using motion-free k-space data only, with no increase in scan time. **Magn Reson Med 70:1332–1339, 2013.** ©2012 Wiley Periodicals, Inc.

Key words: signal-to-noise ratio; diaphragmatic navigators; motion correction; cardiac MRI; coronary MRI; late gadolinium enhancement

INTRODUCTION

Three-dimensional (3D) high-resolution cardiac MRI, such as coronary MRI and late gadolinium enhancement (LGE) imaging, is acquired in a segmented fashion over multiple heartbeats, which necessitates compensation of respiratory and cardiac motions (1). The latter is typically suppressed by imaging during the patient-specific rest period of the cardiac cycle (1,2). For high-resolution 3D sequences, where the acquisition cannot be completed within a single breath-hold, techniques for respiratory motion compensation have been developed. Respiratory navigators (NAVs), which use a two-dimensional pencil beam typically positioned on the dome of the right hemi-diaphragm, have been used to track respiratory motion (3). Due to a linear dependency between the respiratory motion of the heart and that of the right hemi-diaphragm, NAV can be used to indirectly monitor the motion of the heart (4). In prospective NAV gating, the k-space lines acquired immediately after the NAV signal are used for image reconstruction only if the NAV signal is within a predefined gating window (5). Otherwise, the corresponding k-space lines are rejected and reacquired in the next cardiac cycle. For a 5-mm gating window, this typically results in an acceptance efficiency of 30%–70%, where the rejected lines are discarded and not used in reconstruction.

Alternative techniques have been developed to improve the efficiency of respiratory motion compensation. Prospective motion correction has been used in coronary MRI to achieve scan efficiencies of 80%–100% (6,7). Retrospective motion estimation has also been used in coronary MRI to correct for the motion of the rejected lines for 3D radial trajectories with projection-based self-gating (8), and for sequences using image-based NAVs (9,10). Self-gating with radial trajectories has been used in LGE imaging as well (11), but image-based NAVs may not be directly applicable in this case due to the inversion pulse applied before imaging.

Another major challenge in high-resolution cardiac MRI is the limited signal-to-noise ratio (SNR). In coronary MRI, administration of vasodilators (12), imaging at higher magnetic field strengths (13–15), and use of exogenous contrast agents (16–25) have been investigated as means

Department of Medicine, Beth Israel Deaconess Medical Center and Harvard Medical School, Boston, Massachusetts, USA.

Grant sponsor: NIH; Grant numbers: R01EB008743-01A2, K99HL111410-01, and UL1 RR025758-01; Grant sponsor: Samsung Electronics.

*Correspondence to: Reza Nezafat, Ph.D., Beth Israel Deaconess Medical Center, 330 Brookline Ave, Boston, MA 02215. E-mail: rnezafat@bidmc.harvard.edu

Received 23 July 2012; revised 20 October 2012; accepted 26 October 2012.

DOI 10.1002/mrm.24566

Published online 11 December 2012 in Wiley Online Library (wileyonlinelibrary.com).

© 2012 Wiley Periodicals, Inc.

1332

of improving SNR. In LGE imaging, the limited SNR can be increased by imaging over alternate heartbeats (26), thereby allowing more signal regrowth but also doubling the scan time. However, we note that the primary reason for the use of alternate heartbeat imaging technique is robustness against magnetization variations. For two-dimensional LGE imaging with breathhold acquisitions, motion-corrected averaging has been used (27). However, due to long acquisition times and inter-average motion, multiple averages for 3D imaging are rarely used.

In this study, we sought to develop and evaluate a novel technique that uses the NAV-rejected k-space lines, which are not conventionally used for image reconstruction and are discarded, to improve SNR without increasing the acquisition time. We use a 3D translational motion model, which was successfully used in previous high-resolution cardiac MRI studies to reduce motion artifacts (28) and was shown to be the dominant component of affine motion models (7,8). Using this motion model, the maximum-likelihood estimates of the motion parameters and the k-space line are jointly determined from the corresponding accepted and rejected k-space lines. The proposed technique is then evaluated in vivo, using coronary MRI and LGE imaging of the left atrium (LA).

THEORY

We denote the underlying image as $\mathbf{m}(x,y,z)$ and the corresponding k-space as $\mathbf{S}(k_x, k_y, k_z)$. When the underlying object undergoes a translational motion of (x_0, y_0, z_0) , the k-space experiences a phase-shift as

$$\hat{\mathbf{S}}(k_x, k_y, k_z) = e^{-i2\pi k_x x_0 - i2\pi k_y y_0 - i2\pi k_z z_0} \mathbf{S}(k_x, k_y, k_z). \quad [1]$$

Consider a NAV-gated segmented imaging protocol, where the k-space line at (k_x^0, k_y^0, k_z^0) is being acquired. We note that in the following, we will not explicitly write out the dependence on (k_x^0, k_y^0, k_z^0) to simplify the notation. This k-space line is rejected if the NAV detects that the object has moved. In this case, the rejected k-space line is given by:

$$\mathbf{s}^{\text{rej},1} = e^{-i2\pi k_x x_1 - i2\pi k_y y_1 - i2\pi k_z z_1} \circ \mathbf{s} + \mathbf{n}_1, \quad [2]$$

where \mathbf{s} is the vector of values along the read-out (k_x) direction corresponding to the original image $\mathbf{m}(x,y,z)$, $\mathbf{s}^{\text{rej},1}$ is the first rejected k-space line at this k-space location, \mathbf{n}_1 is the measurement noise, (x_1, y_1, z_1) is the motion the object has experienced, \mathbf{k}_x is the vector of values for the extent of the k-space in the read-out direction, and \circ denotes elementwise multiplication. This line will then be reacquired until it is within an acceptable gating window. We denote the k-space line corresponding to the p th time, it is rejected as

$$\mathbf{s}^{\text{rej},p} = e^{-i2\pi k_x x_p - i2\pi k_y y_p - i2\pi k_z z_p} \circ \mathbf{s} + \mathbf{n}_p. \quad [3]$$

As \mathbf{s} only contains measurements along the k_x direction for a fixed (k_y^0, k_z^0) location, the motion in y - z direction cannot be determined individually. Thus, the rejected line can be rewritten as

$$\mathbf{s}^{\text{rej},p} = e^{-i2\pi \mathbf{k}_x x_p - i\theta_p} \circ \mathbf{s} + \mathbf{n}_p, \quad [4]$$

thus reducing the number of unknowns. Similarly, the accepted line is given by

$$\mathbf{s}^{\text{acc}} = \mathbf{s} + \mathbf{n}_{\text{acc}}. \quad [5]$$

Conventional reconstruction fills the k-space, $\mathbf{S}(k_x, k_y, k_z)$ with the accepted lines \mathbf{s}^{acc} for each k-space location (k_y^0, k_z^0) , whereas our goal is to reduce the effect of the noise by using all the available lines. Under an independent identically distributed Gaussian noise assumption, the likelihood function for the unknown variables, \mathbf{s} and $\{x_p, \theta_p\}_{p=1}^{n_{\text{rej}}}$ can be written as

$$L(\mathbf{s}, \{x_p, \theta_p\}_{p=1}^{n_{\text{rej}}}) = -\|\mathbf{s} - \mathbf{s}^{\text{acc}}\|_2^2 - \sum_{p=1}^{n_{\text{rej}}} \|\mathbf{s}^{\text{rej},p} - e^{-i2\pi \mathbf{k}_x x_p - i\theta_p} \circ \mathbf{s}\|_2^2, \quad [6]$$

where n_{rej} is the number of NAV-rejected lines at the given k-space location. The maximum-likelihood estimate is then given by

$$\left(\mathbf{s}^{\text{ML}}, \{x_p^{\text{ML}}, \theta_p^{\text{ML}}\}_{p=1}^{n_{\text{rej}}} \right) = \arg \min_{\mathbf{s}, \{x_p, \theta_p\}_{p=1}^{n_{\text{rej}}}} \|\mathbf{s} - \mathbf{s}^{\text{acc}}\|_2^2 + \sum_{p=1}^{n_{\text{rej}}} \|\mathbf{s}^{\text{rej},p} - e^{-i2\pi \mathbf{k}_x x_p - i\theta_p} \circ \mathbf{s}\|_2^2. \quad [7]$$

We solve the nonlinear least squares problem in Eq. 7 using an alternating minimization approach (29,30). At iteration t , the current estimate $\mathbf{s}^{(t)}$ is held fixed, and for each p

$$\left(x_p^{(t)}, \theta_p^{(t)} \right) = \arg \min_{x_p, \theta_p} \|\mathbf{s}^{\text{rej},p} - e^{-i2\pi \mathbf{k}_x x_p - i\theta_p} \circ \mathbf{s}^{(t)}\|_2^2 \quad [8]$$

is solved. Then, $\{x_p^t, \theta_p^t\}_{p=1}^{n_{\text{rej}}}$ is held fixed, and $\mathbf{s}^{(t+1)}$ is generated as follows

$$\begin{aligned} \mathbf{s}^{(t+1)} &= \arg \min_{\mathbf{s}} \|\mathbf{s} - \mathbf{s}^{\text{acc}}\|_2^2 + \sum_{p=1}^{n_{\text{rej}}} \|\mathbf{s}^{\text{rej},p} - e^{-i2\pi \mathbf{k}_x x_p - i\theta_p} \circ \mathbf{s}\|_2^2 \\ &= \frac{1}{n_{\text{rej}} + 1} \left(\mathbf{s}^{\text{acc}} + \sum_{p=1}^{n_{\text{rej}}} e^{i2\pi \mathbf{k}_x x_p + i\theta_p} \circ \mathbf{s}^{\text{rej},p} \right). \quad [9] \end{aligned}$$

Finally, we note that for two vectors \mathbf{u}, \mathbf{v} , we have $\hat{\theta} = \arg \min_{\theta} \|\mathbf{v} - e^{i\theta} \mathbf{u}\|_2^2 = \angle(\mathbf{u} * \mathbf{v})$. Thus, to solve Eq. 8, first the θ potential displacements, x_j are quantized between x_{min} and x_{max} with step size x_{step} . Then, for each value of x_j in this set, the corresponding θ_j is calculated as $\angle((e^{i2\pi \mathbf{k}_x x_j} \circ \mathbf{s}^{\text{rej},p}) * \mathbf{s}^{(t)})$. Then, Eq. 8 is minimized over the set of parameters for x_p . This approach reduces the search space to only the x direction, and avoids quantization for θ .

METHODS

Imaging Studies

All imaging was performed on a 1.5-T Philips Achieva (Philips Healthcare, Best, the Netherlands) system with a

32-channel cardiac phased-array receiver coil. For this HIPAA-compliant study, the imaging protocol was approved by our institutional review board, and written informed consent was obtained from all participants.

Coronary MRI in Healthy Subjects

Ten healthy adult subjects (eight females, 26.6 ± 9.8 years) without contraindications to MRI were recruited for left anterior descending (LAD) coronary artery imaging. Scout images were acquired with a steady-state free precession sequence with in-plane resolution 3.1×3.1 mm² and 10 mm slice thickness. This was followed by an image set acquired with an axial breathhold cine steady-state free precession sequence (pulse repetition time/echo time = 3.7/1.85 ms; temporal resolution, 48 ms; spatial resolution 1.7×1.7 mm²; acceleration rate, two) to visually identify the quiescent period of the LAD. The corresponding trigger delay was used for coronary acquisition. A low-resolution coronary survey 3D volume was then acquired for localization and assignment of the appropriate imaging slab. A free-breathing electrocardiogram-triggered NAV-gated steady-state free precession sequence was used for acquisition. The imaging parameters were pulse repetition time/echo time = 4.3/2.1 ms, flip angle = 90°, field of view = $270 \times 270 \times 30$ mm³, spatial resolution = $1.0 \times 1.0 \times 3.0$ mm³. A spectrally selective fat-saturation sequence and T₂ magnetization preparation were used to improve contrast (31). A NAV placed on the dome of the right hemi-diaphragm was used for respiratory motion compensation, using prospective real-time correction with a 5-mm end-expiration gating window and 0.6 superior–inferior tracking ratio (4,32). All images were acquired axially with right-left phase encoding. Saturation bands were placed over the stationary tissues to reduce artifacts along the phase encode direction.

LA LGE in Patients

Twenty-one patients (eight females, 60.8 ± 8.6 years) referred for assessment of LA anatomy before or post pulmonary vein isolation (PVI) were recruited for LA LGE imaging. All patients had a history of atrial fibrillation and no contraindications to MRI. Sixteen were imaged before PVI, and five post-PVI. All subjects were in sinus rhythm. LGE images were acquired 10–20 min after a bolus (2 mL/s) infusion of 0.1 mmol/kg of Gd-BOPTA (MultiHance, Bracco, Rome, Italy). The optimal inversion time was selected to null the left ventricular myocardial signal using a Look-Locker sequence. A free-breathing electrocardiogram-triggered NAV-gated inversion-recovery gradient echo imaging sequence was used for all acquisitions. The imaging parameters were pulse repetition time/echo time = 5.2/2.6 ms, flip angle = 25°, field-of-view = $320 \times 400 \times 90$ mm³, spatial resolution = $1.4 \times 1.4 \times 4.0$ mm³. A respiratory NAV placed on the dome of the right hemi-diaphragm was used for respiratory motion compensation, using an end-expiration adaptive gating window strategy with a target efficiency varying between 40% and 50% (33). This corresponded to an average gating window of 8.2 ± 3.6 mm. Saturation

bands were placed over the stationary tissues. All imaging was performed axially with right-left phase-encoding to reduce respiratory artifacts from the chest wall.

Image Reconstruction

The k-space data were exported and transferred to a stand-alone workstation for further analysis. The proposed method was implemented in Matlab (v7.6, MathWorks, Natick, MA). For all datasets, the proposed motion correction for improved SNR was performed for each coil independently. The parameters for the displacement in the x direction was chosen as $x_{\text{step}} = 0.2$ pixels, $x_{\text{min}} = -10$ pixels, and $x_{\text{max}} = 10$ pixels. The alternating minimization procedure was performed for five iterations. Comparison images were generated via the conventional technique of using only the NAV-accepted data, as well as using simple averaging of accepted and motion-corrupted lines. In all cases, the final images were generated by root-sum-squares of the individual coil images.

Image and Statistical Analysis

For coronary MRI, objective vessel sharpness and SNR measurements were used to evaluate the conventional and proposed reconstructions for all datasets. SNR measurements were performed using Matlab (v7.6, MathWorks, Natick, MA) on the raw images. For coronary MRI, the mean signal intensity of the ascending aorta at the level that the left main coronary artery branches off was measured by drawing a region-of-interest (~ 10 mm radius) for both reconstructions. For LA LGE, the mean signal intensity was measured in the LA and right atrium (RA) blood pools. Noise was measured in the nonsignal areas of each image using a larger region-of-interest. SNR was calculated as the ratio of the mean signal to the standard deviation of the noise. SNR gain was calculated as the ratio of the SNRs of the proposed and conventional techniques. This was compared with the maximum theoretical SNR gain, defined as the theoretical SNR if a given k-space line was acquired $n_{\text{rej}} + 1$ times without undergoing any motion, where n_{rej} is the number of times this line was rejected due to NAV in the original acquisition. A SoapBubble tool (34) was used to quantitatively evaluate LAD vessel sharpness. Vessel sharpness scores were calculated for both sides of the vessel using a Deriche algorithm (35). Final normalized sharpness was defined as the average score of both sides divided by the center of vessel intensity.

A qualitative assessment of image quality was also performed for all images. Left coronary MRI and LGE images were written into DICOM format and imported into ViewForum (Philips Healthcare, Best, NL, vR4.2V1L2) for qualitative evaluation by a blinded reviewer with > 10 years of experience without reformatting. For coronary MRI, separate scores were given to left main, proximal LAD, mid LAD, proximal left circumflex, and proximal right coronary artery. These scores were then combined for statistical analysis. For LA LGE, subjective scores were given for overall image quality of the axial images. For all images, scores were also given for

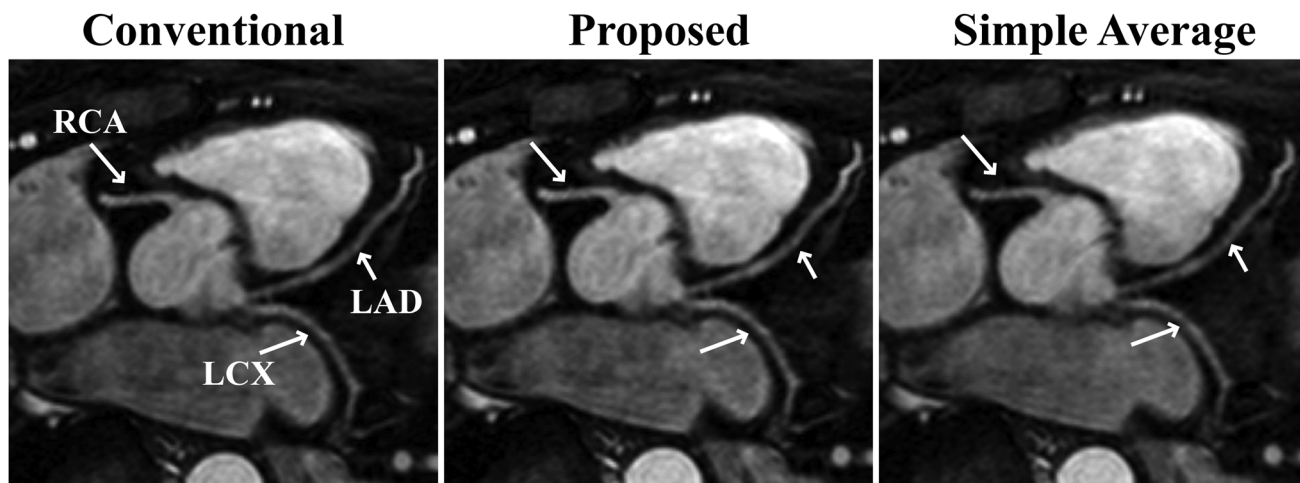


FIG. 1. Reformatted axial slices from a left coronary MRI scan, depicting the LAD, left circumflex, and right coronary artery of a healthy subject, using the conventional image reconstruction with only NAV-accepted data (conventional), the proposed technique, and simple averaging of all data. Coronary arteries are visualized similarly for the conventional and proposed; however, images generated with the proposed technique have 11% higher SNR due to the usage of the NAV-rejected k-space lines. Slight blurring is noticeable in the proximal right coronary artery, mid LAD, and mid left circumflex for the simple averaging, even though its SNR is the same as the proposed technique.

freedom from motion artifacts. All scores were given on a four-point scale (1 = poor, 2 = fair, 3 = good, and 4 = excellent). Additionally, a dichotomous score (yes/no) was noted on the diagnostic quality of the LA LGE images.

Imaging scores, normalized vessel sharpness, and SNR are presented as mean \pm one standard deviation. The signed rank test was used for imaging scores to test for the null hypothesis that the central tendency of the difference was zero for the two reconstructions. All statistical analyses were performed using SAS (v9.3, SAS Institute, Cary, NC). SNR and normalized sharpness scores were compared using the paired *t*-test. A *P* value of < 0.05 was considered to be significant.

RESULTS

Left coronary MRI and LA LGE imaging were successfully completed in all subjects without complications, with an average gating efficiency of $51.5 \pm 8.5\%$ and $42.9 \pm 4.7\%$, respectively. Figure 1 shows reformatted axial images of left coronaries from a healthy subject, reconstructed using the conventional, proposed, and simple averaging methods. The conventional and proposed images are similar in terms of visualization and sharpness, although the proposed technique has 11% higher SNR. The simple averaging technique also yields higher SNR; however, blurring is observed in the proximal right coronary artery, mid LAD, and mid left circumflex branches. Figure 2 shows an example axial slice of LA LGE from a patient who underwent PVI for treatment of atrial fibrillation, reconstructed using the conventional, proposed, and simple averaging methods. The enhancement on the LA wall is visualized similarly using both conventional and proposed techniques. However, for this patient, the proposed technique has 32%–39% higher SNR compared with the conventional technique. The simple averaging technique suffers from blur-

ring of the enhancement region, even though it also yields a higher SNR.

Table 1 summarizes the SNR measurements of the ascending aorta and the corresponding SNR gain, and normalized vessel sharpness measurements for left coronary MRI, as well as the SNR measurements of the LA and the RA, and the respective SNR gains. For the left coronary MRI, there was a significant difference between the SNR of the proposed method and the conventional method (42.7 ± 10.6 vs. 36.6 ± 10.2 , $P < 0.01$), and between the simple averaging method and the conventional method (42.6 ± 10.7 vs. 36.6 ± 10.2 , $P < 0.01$) but no difference between simple averaging and the proposed method ($P = 0.49$). There was no difference in terms of the normalized vessel sharpness between the proposed and conventional methods (0.455 ± 0.075 vs. 0.463 ± 0.063 , $P = 0.19$), but there was a significant difference between simple averaging and conventional methods (0.441 ± 0.069 vs. 0.463 ± 0.063 , $P < 0.01$), and between simple averaging and proposed method ($P = 0.02$). The SNR gain of the proposed method (1.17 ± 0.07) and the maximum theoretical SNR gain (1.19 ± 0.09) were also not statistically different ($P = 0.12$). For LA LGE, there were significant differences in terms of the SNR for the proposed and the conventional techniques, measured in both LA (27.9 ± 14.2 vs. 22.7 ± 11.1 , $P < 0.01$) and RA (31.4 ± 16.1 vs. 25.7 ± 13.2 , $P < 0.01$). The SNR gain of the proposed method (1.21 ± 0.09 as measured in the LA, 1.22 ± 0.09 as measured in the RA) and the maximum theoretical SNR gain (1.24 ± 0.07) were not statistically different ($P = 0.11$ and $P = 0.25$, respectively). The same results hold for the SNR behavior of the simple averaging technique as expected.

Table 2 depicts the qualitative scores for overall image quality and freedom from motion artifacts for left coronary MRI and LA LGE, as well as presence of enhancement in LA LGE. There were no differences among the proposed and conventional techniques in terms of

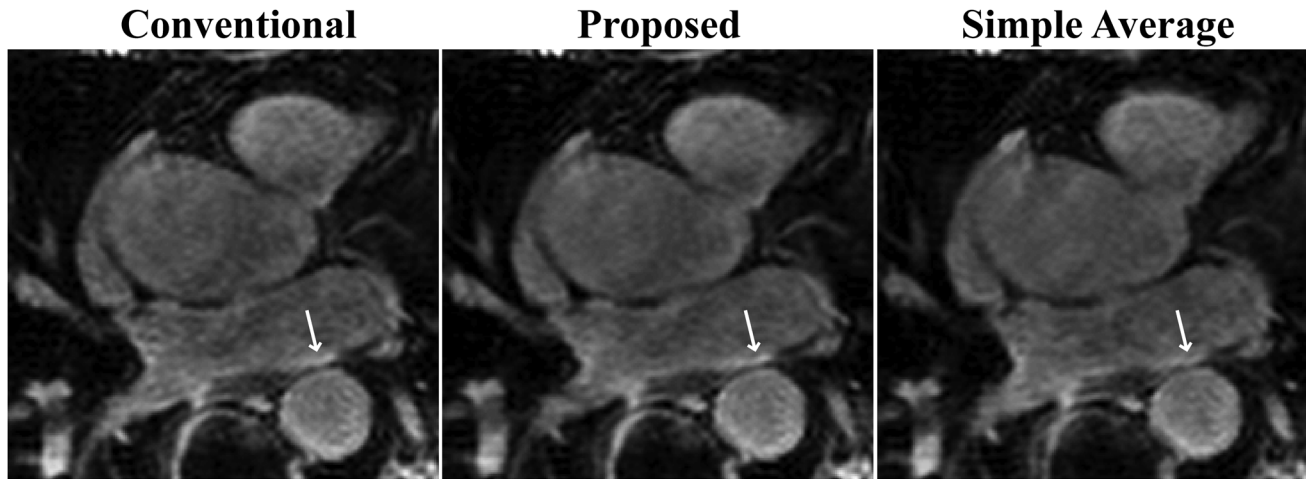


FIG. 2. An example axial slice from a patient who underwent PVI for treatment of atrial fibrillation, reconstructed using the conventional technique with only NAV-accepted data (conventional), the proposed technique, and simple averaging of all data. Conventional and proposed images both show the enhancement of the left atrial (LA) wall (arrows) and are structurally similar. The image generated with the proposed technique has 32% higher SNR in the LA blood pool and 39% higher SNR in the RA blood pool. Although the SNR of the simple averaging technique is also higher, it suffers from blurring in the enhancement due to averaging of motion.

overall image quality and the presence of motion artifacts for both coronary MRI ($P = 0.50$ and $P = 1.00$, respectively) and LA LGE ($P = 1.00$ and $P = 1.00$, respectively). However, for left coronary MRI, the image quality of simple averaging was significantly different than both techniques ($P < 0.01$ for both), even though there was no significant difference in terms of motion artifacts ($P = 1.00$ for both). For LA LGE, the presence of motion artifacts with the simple averaging technique was significantly worse than both other techniques ($P < 0.01$), even though the overall image quality was not different ($P = 0.25$). Furthermore, there was no disagreement between any techniques in terms of detection of enhancement for LA LGE.

DISCUSSION

In this study, we have proposed and evaluated an image reconstruction technique that is associated with improved SNR that uses information from NAV-rejected k-space lines for high-resolution free-breathing MRI acquisitions. These rejected k-space lines are conventionally discarded and not used in image reconstruction. Thus, our technique is able to improve SNR without

requiring additional acquisition time. Furthermore, it does not suffer from additional artifacts or blurriness.

There are significant variations in breathing patterns of subjects. This is manifested not only in terms of differences in gating efficiency but also in terms of how many times each line is reacquired until it is accepted. For healthy subjects, the maximum number of reacquisitions at any given k-space location among all our scans is 26, whereas for the patients, this number goes up to 61. This difference in the number of times each k-space line is reacquired leads to a nontrivial relationship between the SNR gain and the navigating efficiency. Hence, a 50% gating efficiency does not translate to $\sqrt{2}$ gain in SNR. The variation in the breathing pattern may also result in rejected k-space lines that are well out of the gating window. Image quality may be further improved by only using rejected k-space lines within a larger gating window (e.g., 15 mm) in the proposed technique. The larger gating window may be retrospectively applied using NAV data. We note that this approach was not explored in this study due to the lack of NAV data at the time of our study, although the inclusion of all rejected k-space lines did not deteriorate the image quality.

Table 1

Comparison of Signal-To-Noise-Ratio (SNR) and SNR Gain between the Conventional, Proposed and Simple Averaging Techniques for Left Coronary MRI and for Left Atrium (LA) Late Gadolinium Enhancement (LGE), as well as the Normalized Vessel Sharpness Measurements for Left Coronary MRI

	Left coronary MRI			LA LGE			
	Vessel sharpness	SNR	SNR gain	SNR (LA)	SNR gain	SNR (RA)	SNR gain
Conventional	0.463 ± 0.063	36.6 ± 10.2	1.00 ± 0.00	22.7 ± 11.1	1.00 ± 0.00	25.7 ± 13.2	1.00 ± 0.00
Proposed	0.455 ± 0.075	42.7 ± 10.6	1.17 ± 0.07	27.9 ± 14.2	1.21 ± 0.09	31.4 ± 16.1	1.22 ± 0.09
Simple average	0.441 ± 0.069	42.6 ± 10.7	1.17 ± 0.07	27.9 ± 14.1	1.21 ± 0.09	31.5 ± 16.2	1.22 ± 0.99

The proposed technique and simple averaging significantly improves SNR for left coronary MRI as measured in the ascending aorta, and for LA LGE as measured in the LA and the right atrium (RA) ($P < 0.01$ for all cases). There were no significant differences between vessel sharpness measurements and imaging scores between conventional and proposed technique ($P = 0.49$). However, significant differences were observed between simple averaging and both other techniques ($P < 0.01$ for both).

Table 2

Subjective Image Scores and Freedom From Motion Scores (1 = poor, 2 = fair, 3 = good, 4 = excellent) for the Conventional, Proposed and Simple Averaging Reconstruction Techniques for Left Coronary MRI and for LA LGE

	Left Coronary MRI		LA LGE		
	Image score	Freedom from motion	Image score	Freedom from motion	Presence of LGE
Conventional	2.88 ± 1.08	2.90 ± 0.99	3.00 ± 0.71	3.57 ± 0.60	6/21
Proposed	2.84 ± 1.13	2.90 ± 0.99	3.00 ± 0.71	3.57 ± 0.60	6/21
Simple average	2.62 ± 1.12	2.80 ± 0.92	2.86 ± 0.79	3.05 ± 0.80	6/21

There are no significant differences between the proposed and conventional techniques in terms of overall image quality or motion artifacts both in coronary MRI and LA LGE ($P = 0.50, 1.00, 1.00, 1.00$ respectively). However, for coronary MRI, the image quality of simple averaging was significantly worse than both techniques ($P < 0.01$ for both), though there was no difference in terms of motion artifacts ($P = 1.00$ for both). For LA LGE, the presence of motion artifacts with the sample averaging technique was significantly worse than both other techniques ($P < 0.01$), even though the overall image quality was not different ($P = 0.25$). There is no disagreement between the techniques in terms of detection of enhancement in LA LGE.

Even though a small gating window is used in our acquisitions, there will be motion within the gating window over multiple segments. In conventional imaging, this motion is assumed to be negligible, and the k-space data from various segments are combined to form the final image. In our approach, we also assume the accepted line is motion-free, and the maximum-likelihood estimate is calculated based on this assumption. Inclusion of motion between different segments would require the combined processing of all k-space lines, as well as a model for motion uncertainty, which would lead to prohibitively large problem size. Thus, the motion within the gating window was not considered in this study.

The proposed technique was used in imaging sequences with low SNR. LGE imaging has an inherently low SNR due to the application of an inversion pulse and lack of recovery. Additionally, the presence of gadolinium affects the contrast of the k-space lines acquired over time. Thus, if a line is rejected and reacquired, the contrast will not be exactly same due to the changing inversion time and effects of contrast wash-out. This issue was not noted in our study. However, this phenomenon may create contrast differences between the conventional and the proposed technique, if central k-space lines are rejected and reacquired over multiple heart cycles.

The images generated with the simple averaging technique were qualitatively different for the two sequences on two different cohorts. In the coronary artery imaging of healthy subjects, no significant differences were observed in terms of motion artifacts. One possible explanation for this is the regular breathing pattern of the healthy subject population averages itself out and does not create severe motion artifacts even without motion correction. However, subtle changes in sharpness of the vessels were observed by the experienced blinded reader, leading to a lower image quality score. On the other hand, in LA LGE imaging of patients, which has coarser resolution and where the diagnostic value of the images is largely based on the delineation of scar, the image quality was not significantly different than the other two techniques. However, the motion artifacts in this case were more notable, as this cohort is likely to have a more irregular breathing pattern than the healthy subjects. Finally, we note that simple averaging still uses

information from accepted k-space lines to average out motion artifacts, and thus it is fundamentally different than an acquisition strategy where no gating is used.

The reconstruction time of the MATLAB implementation of the proposed algorithm was ~ 18 ms per k-space line, although the exact value depends on the number of rejected acquisitions for that line. Although this reconstruction time is not substantial, this particular implementation is unlikely to be used in real-time due to the need of reconstructing multiple coil data for multiple k-space lines per segment. Thus, for real-time reconstruction, alternative reconstruction techniques based on other programming languages or parallel implementations on graphics processing units (36) may be necessary.

In our imaging sequences, saturation bands were used to suppress the signal from stationary tissues, such as arms and the back. Thus, the majority of the signal in each coil comes from the moving objects, and the acquired k-space lines can be corrected for translational motion. In cases, where the stationary tissues are not suppressed, these stationary tissues may need to be segmented out, and their signal contribution may need to be subtracted out from individual k-space lines before applying motion correction. We also note that in segmented acquisitions of high-resolution cardiac MRI, the application of saturation bands, as was done in our study, does not increase the scan time, as imaging can only be performed during the rest period of the heart cycle.

Although rejected k-space lines are not used for SNR improvement in prior work, there are a number of approaches that aim to correct the motion in lines using additional information, such as two-dimensional or 3D NAVs (9,28,37,38), self-navigating approaches (39,40), or binning strategies based on NAV data (8) for improved scan efficiency. Our approach is fundamentally different than these techniques, as the proposed technique requires no additional information than the accepted and rejected k-space lines. However, due to the presence of the accepted k-space line in maximum-likelihood estimation, our technique cannot be used directly for improved scan efficiency.

SNR increases for both coronary MRI and LGE have been reported when imaging at higher fields (41,42). Although SNR increases between 30% and 60% have

been reported (42–46), these differences in SNR have not translated to improved diagnostic quality (47,48). This is consistent with the findings in our study, where the improved SNR did not result in improved imaging scores. It may be possible to use the improved SNR for higher spatial resolution; however, this was not studied.

CONCLUSION

We have demonstrated a technique that uses NAV-rejected k-space lines for improved SNR without resulting in a longer acquisition or imaging artifacts.

ACKNOWLEDGMENTS

The authors thank Warren J. Manning, MD for his editorial comments.

REFERENCES

- Scott AD, Keegan J, Firmin DN. Motion in cardiovascular MR imaging. *Radiology* 2009;250:331–351.
- Wang Y, Vidan E, Bergman GW. Cardiac motion of coronary arteries: variability in the rest period and implications for coronary MR angiography. *Radiology* 1999;213:751–758.
- Ehman RL, Felmlee JP. Adaptive technique for high-definition MR imaging of moving structures. *Radiology* 1989;173:255–263.
- Wang Y, Riederer SJ, Ehman RL. Respiratory motion of the heart: kinematics and the implications for the spatial resolution in coronary imaging. *Magn Reson Med* 1995;33:713–719.
- Oshinski JN, Hofland L, Mukunda SJ, Dixon WT, Parks WJ, Pettigrew RI. Two-dimensional coronary MR angiography without breath holding. *Radiology* 1996;201:737–743.
- Manke D, Nehrke K, Bornert P. Novel prospective respiratory motion correction approach for free-breathing coronary MR angiography using a patient-adapted affine motion model. *Magn Reson Med* 2003;50:122–131.
- Nehrke K, Bornert P. Prospective correction of affine motion for arbitrary MR sequences on a clinical scanner. *Magn Reson Med* 2005;54:1130–1138.
- Bhat H, Ge L, NIELLES-VALLESPIN S, ZUEHLSORFF S, LI D. 3D radial sampling and 3D affine transform-based respiratory motion correction technique for free-breathing whole-heart coronary MRA with 100% imaging efficiency. *Magn Reson Med* 2011;65:1269–1277.
- Schmidt JF, Buehrer M, Boesiger P, Kozerke S. Nonrigid retrospective respiratory motion correction in whole-heart coronary MRA. *Magn Reson Med* 2011;66:1541–1549.
- Henningson M, Koken P, Stehning C, Razavi R, Prieto C, Botnar RM. Whole-heart coronary MR angiography with 2D self-navigated image reconstruction. *Magn Reson Med* 2012;67:437–445.
- Adluru G, Chen L, Kim S-E, Kholmovski E, Marrouche NF, DiBella EV. Self-navigated 3D late gadolinium enhancement imaging of the left atrium. In Proceedings of the 19th Annual Meeting of ISMRM, Montreal, May 2011. p. 1378.
- Hu P, Chuang ML, Ngo LH, Stoeck CT, Peters DC, Kissinger KV, Goddu B, Goepfert LA, Manning WJ, Nezafat R. Coronary MR imaging: effect of timing and dose of isosorbide dinitrate administration. *Radiology* 2010;254:401–409.
- Nezafat R, Ouwerkerk R, Derbyshire AJ, Stuber M, McVeigh ER. Spectrally selective B1-insensitive T2 magnetization preparation sequence. *Magn Reson Med* 2009;61:1326–1335.
- van Elderen SG, Versluis MJ, Westenberg JJ, Agarwal H, Smith NB, Stuber M, de Roos A, Webb AG. Right coronary MR angiography at 7 T: a direct quantitative and qualitative comparison with 3 T in young healthy volunteers. *Radiology* 2010;257:254–259.
- Gharib AM, Abd-Elmoniem KZ, Herzka DA, Ho VB, Locklin J, Tzatha E, Stuber M, Pettigrew RI. Optimization of coronary whole-heart MRA free-breathing technique at 3 Tesla. *Magn Reson Imaging* 2011;29:1125–1130.
- Knuesel PR, Nanz D, Wolfensberger U, Saranathan M, Lehning A, Luescher TF, Marincek B, von Schulthess GK, Schwitler J. Multislice breath-hold spiral magnetic resonance coronary angiography in patients with coronary artery disease: effect of intravascular contrast medium. *J Magn Reson Imaging* 2002;16:660–667.
- Paetsch I, Jahnke C, Barkhausen J, Spuentrup E, Cavagna F, Schnackenburg B, Huber M, Stuber M, Fleck E, Nagel E. Detection of coronary stenoses with contrast enhanced, three-dimensional free breathing coronary MR angiography using the gadolinium-based intravascular contrast agent gadocoletic acid (B-22956). *J Cardiovasc Magn Reson* 2006;8:509–516.
- Prompona M, Cyran C, Nikolaou K, Bauner K, Reiser M, Huber A. Contrast-enhanced whole-heart MR coronary angiography at 3.0 T using the intravascular contrast agent gadofosveset. *Invest Radiol* 2009;44:369–374.
- Goldfarb JW, Edelman RR. Coronary arteries: breath-hold, gadolinium-enhanced, three-dimensional MR angiography. *Radiology* 1998;206:830–834.
- Zheng J, Bae KT, Woodard PK, Haacke EM, Li D. Efficacy of slow infusion of gadolinium contrast agent in three-dimensional MR coronary artery imaging. *J Magn Reson Imaging* 1999;10:800–805.
- Li D, Carr JC, Shea SM, Zheng J, Deshpande VS, Wielopolski PA, Finn JP. Coronary arteries: magnetization-prepared contrast-enhanced three-dimensional volume-targeted breath-hold MR angiography. *Radiology* 2001;219:270–277.
- Weber OM, Martin AJ, Higgins CB. Whole-heart steady-state free precession coronary artery magnetic resonance angiography. *Magn Reson Med* 2003;50:1223–1228.
- Bi X, Carr JC, Li D. Whole-heart coronary magnetic resonance angiography at 3 Tesla in 5 minutes with slow infusion of Gd-BOPTA, a high-relaxivity clinical contrast agent. *Magn Reson Med* 2007;58:1–7.
- Hu P, Chan J, Ngo LH, et al. Contrast-enhanced whole-heart coronary MRI with bolus infusion of gadobenate dimeglumine at 1.5 T. *Magn Reson Med* 2011;65:392–398.
- Akçakaya M, Basha TA, Chan RH, Rayatzadeh H, Kissinger KV, Goddu B, Goepfert LA, Manning WJ, Nezafat R. Accelerated contrast-enhanced whole-heart coronary MRI using low-dimensional-structure self-learning and thresholding. *Magn Reson Med* 2012;67:1434–1443.
- Kellman P, Arai AE, McVeigh ER, Aletras AH. Phase-sensitive inversion recovery for detecting myocardial infarction using gadolinium-delayed hyperenhancement. *Magn Reson Med* 2002;47:372–383.
- Ledesma-Carbayo MJ, Kellman P, Hsu LY, Arai AE, McVeigh ER. Motion corrected free-breathing delayed-enhancement imaging of myocardial infarction using nonrigid registration. *J Magn Reson Imaging* 2007;26:184–190.
- Keegan J, Gatehouse PD, Yang GZ, Firmin DN. Non-model-based correction of respiratory motion using beat-to-beat 3D spiral fat-selective imaging. *J Magn Reson Imaging* 2007;26:624–629.
- Lee DD, Seung HS. Algorithms for non-negative matrix factorization. In Proceedings Advances In Neural Information Processing Systems, Vancouver, Canada, 2001. p. 556–562.
- Berry MW, Browne M, Langville AN, Puaça VP, Plemmons RJ. Algorithms and applications for approximate nonnegative matrix factorization. *Comput Statist Data Anal* 2007;52:155–173.
- Brittain JH, Hu BS, Wright GA, Meyer CH, Macovski A, Nishimura DG. Coronary angiography with magnetization-prepared T2 contrast. *Magn Reson Med* 1995;33:689–696.
- Danias PG, Stuber M, Botnar RM, Kissinger KV, Edelman RR, Manning WJ. Relationship between motion of coronary arteries and diaphragm during free breathing: lessons from real-time MR imaging. *AJR* 1999;172:1061–1065.
- Moghari MH, Chan RH, Hong SN, Shaw JL, Goepfert LA, Kissinger KV, Goddu B, Josephson ME, Manning WJ, Nezafat R. Free-breathing cardiac MR with a fixed navigator efficiency using adaptive gating window size. *Magn Reson Med* 2012;68:1866–1875.
- Etienne A, Botnar RM, Van Muiswinkel AM, Boesiger P, Manning WJ, Stuber M. “Soap-Bubble” visualization and quantitative analysis of 3D coronary magnetic resonance angiograms. *Magn Reson Med* 2002;48:658–666.
- Deriche R. Fast algorithms for low-level vision. *IEEE Trans Pattern Anal Mach Intell* 1990;12:78–87.
- Nam S, Akçakaya M, Basha TA, Stehning C, Manning WJ, Tarokh V, Nezafat R. Compressed Sensing reconstruction for whole heart imaging with 3D radial trajectories: a GPU implementation. *Magn Reson Med* 2012. doi: 10.1002/mrm.24280.
- Lai P, Bi X, Jerecic R, Li D. A respiratory self-gating technique with 3D-translation compensation for free-breathing whole-heart coronary MRA. *Magn Reson Med* 2009;62:731–738.
- Henningson M, Smink J, Razavi R, Botnar RM. Prospective respiratory motion correction for coronary MR angiography using a 2D image navigator. *Magn Reson Med* 2013;69:486–494.

39. Larson AC, White RD, Laub G, McVeigh ER, Li D, Simonetti OP. Self-gated cardiac cine MRI. *Magn Reson Med* 2004;51:93–102.
40. Lai P, Larson AC, Park J, Carr JC, Li D. Respiratory self-gated four-dimensional coronary MR angiography: a feasibility study. *Magn Reson Med* 2008;59:1378–1385.
41. Gharib AM, Elagha A, Pettigrew RI. Cardiac magnetic resonance at high field: promises and problems. *Curr Probl Diagn Radiol* 2008;37:49–56.
42. Gutberlet M, Noeske R, Schwinge K, Freyhardt P, Felix R, Niendorf T. Comprehensive cardiac magnetic resonance imaging at 3.0 Tesla: feasibility and implications for clinical applications. *Invest Radiol* 2006;41:154–167.
43. Klumpp B, Fenchel M, Hoewelborn T, Helber U, Scheule A, Claussen C, Miller S. Assessment of myocardial viability using delayed enhancement magnetic resonance imaging at 3.0 Tesla. *Invest Radiol* 2006;41:661–667.
44. Stuber M, Botnar RM, Fischer SE, Lamerichs R, Smink J, Harvey P, Manning WJ. Preliminary report on in vivo coronary MRA at 3 Tesla in humans. *Magn Reson Med* 2002;48:425–429.
45. Botnar RM, Stuber M, Lamerichs R, Smink J, Fischer SE, Harvey P, Manning WJ. Initial experiences with in vivo right coronary artery human MR vessel wall imaging at 3 tesla. *J Cardiovasc Magn Reson* 2003;5:589–594.
46. Bi X, Deshpande V, Simonetti O, Laub G, Li D. Three-dimensional breathhold SSFP coronary MRA: a comparison between 1.5T and 3.0T. *J Magn Reson Imaging* 2005;22:206–212.
47. Klumpp BD, Sandstede J, Lodemann KP, Seeger A, Hoewelborn T, Fenchel M, Kramer U, Claussen CD, Miller S. Intraindividual comparison of myocardial delayed enhancement MR imaging using gadobenate dimeglumine at 1.5 T and 3 T. *Eur Radiol* 2009;19:1124–1131.
48. Ligabue G, Fiocchi F, Ferraresi S, Barbieri A, Rossi R, Modena MG, Romagnoli R, Torricelli P. 3-Tesla MRI for the evaluation of myocardial viability: a comparative study with 1.5-Tesla MRI. *Radiol Med* 2008;113:347–362.